

Dispersion Characteristics of Anisotropic Coupled Circuits with Arbitrarily Located Metallic Strips in Multilayer Configuration

M. L. Tounsi

Faculty of Electronics and Informatics
U.S.T.H.B University, Algiers, Algeria
email : mltounsi@iee.org

A. Khodja

Instrumentation Laboratory,
Faculty of Electronics and Informatics
U.S.T.H.B University, Algiers, Algeria

M.C.E. Yagoub

EECS, University of Ottawa,
800 King Edward,
Ottawa, Ontario, Canada

Abstract –In this paper, a fullwave-mode analysis method is proposed for analyzing the dispersion properties of anisotropic coupled microstrip circuits with arbitrary located metallic strips in multilayer configuration. The numerical procedure is based on a spectral domain approach via an adequate choice of basis functions for current densities on the strips. The proposed model should be useful in computer-aided design of such structures in ultra-wide band (UWB) and millimeter-wave applications. Numerical results are in good agreement with data available in the literature.

Keywords- multilayer; anisotropy; spectral technique; dispersion.

I. INTRODUCTION

In microwave and optical regions, several techniques and technologies have been well developed, leading to various applications in radar, communications and other commercial sectors. The growing interest for coupled structures in microwave integrated circuits applications has considerably increased recently due to their various applications in microwave frequencies including UWB band (3.1-10.6 GHz) to build mixers, modulators, filters and other specific circuits.

Layers of suitable materials may be added to improve the performance of a device or may be required as essential building blocks in the design of a component. For example, in suspended microstrip couplers, extra-layers of dielectrics may be used to improve directivity, very useful in filter design [1]. The analysis of such coupled structures is complicated by the inhomogeneous nature of the problem. The analysis method depends on a number of considerations, such as efficiency, accuracy, memory requirement and versatility.

Anisotropic coupled microstrip-type structures with arbitrary located strips are the most popular circuit elements in microwave integrated circuits (MICs) since they are useful in many practical applications due to their flexibility in the design process and easier matching to external element connections [2]. In such coupled structures, the propagation is described in terms of C- and π -modes [3], which correspond to in-phase and out-of-phase modes, respectively. As mentioned, the analysis of such coupled structures is complex due to the inhomogeneous nature of the problem.

In this paper, the authors propose an original approach that combines speediness and accuracy to efficiently

characterize coupled circuits with arbitrary located strips as well as in arbitrary multilayer configuration by the well-known spectral domain approach (SDA) method using the Galerkin's procedure via a suitable choice of basis functions.

This paper is organized as follows. In Section 2 we discuss the hybrid-mode spectral domain approach for asymmetric anisotropic coupled structures in multilayer configuration. Numerical results are presented in Section 3. Finally we summarize our major results and outline our future work.

II. FORMULATION OF THE METHOD

To illustrate the adopted numerical procedure used to evaluate the model dispersion parameters, we considered a shielded coupled microstrip structure with different widths (w_1 not necessary equal to w_2) in multilayer configuration (Figure 1). The number of layers can be arbitrarily set.

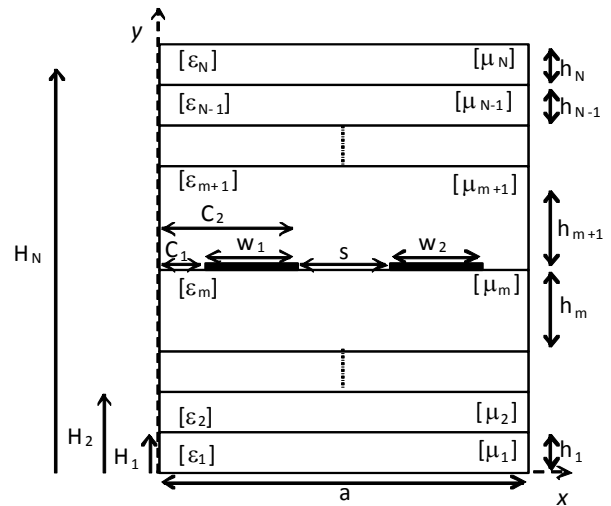


Figure 1. Cross section of an anisotropic microstrip coupler with arbitrary located strips in multilayer configuration

All dielectric layers are assumed anisotropic and lossless. Each layer i ($i = 1 \dots N$) is characterized by its own permittivity $[\epsilon_i]$ and permeability $[\mu_i]$ as

$$[\epsilon_i] = \begin{bmatrix} \epsilon_{xi} & 0 & 0 \\ 0 & \epsilon_{yi} & 0 \\ 0 & 0 & \epsilon_{zi} \end{bmatrix} \quad [\mu_i] = \begin{bmatrix} \mu_{xi} & 0 & 0 \\ 0 & \mu_{yi} & 0 \\ 0 & 0 & \mu_{zi} \end{bmatrix}$$

To get the dispersion characteristics, the spectral domain immittance approach technique [4] was used in

multilayer configuration [5]. The immittance approach allows obtaining the Green's functions via a recursive process based on the determination of the equivalent admittances at all dielectric interfaces H_i ($i=1 \dots N$).

Because the propagation modes are hybrid in a fullwave analysis, the EM field components have been evaluated in each dielectric layer assuming that the hybrid mode is the superposition of LSE ($E_y=0$) and LSM ($H_y=0$) modes. So, the transverse EM field components in the Fourier domain can be expressed as

$$\tilde{H}_{xi} = -\beta \frac{\omega \epsilon_{yi}}{(\alpha_n^2 + \beta^2)} \tilde{E}_{yi} - j\alpha_n \frac{\mu_{yi}}{\mu_{ci}(\alpha_n^2 + \beta^2)} \frac{\partial \tilde{H}_{yi}}{\partial y} \quad (1a)$$

$$\tilde{H}_{zi} = \alpha_n \frac{\omega \epsilon_{yi}}{(\alpha_n^2 + \beta^2)} \tilde{E}_{yi} - j\beta \frac{\mu_{yi}}{\mu_{ci}(\alpha_n^2 + \beta^2)} \frac{\partial \tilde{H}_{yi}}{\partial y} \quad (1b)$$

$$\tilde{E}_{xi} = -j\alpha_n \frac{\epsilon_{yi}}{\epsilon_{ci}(\alpha_n^2 + \beta^2)} \frac{\partial \tilde{E}_{yi}}{\partial y} + \beta \frac{\omega \mu_{yi}}{(\alpha_n^2 + \beta^2)} \tilde{H}_{yi} \quad (1c)$$

$$\tilde{E}_{zi} = -j\beta \frac{\epsilon_{yi}}{\epsilon_{ci}(\alpha_n^2 + \beta^2)} \frac{\partial \tilde{E}_{yi}}{\partial y} - \alpha_n \frac{\omega \mu_{yi}}{(\alpha_n^2 + \beta^2)} \tilde{H}_{yi} \quad (1d)$$

where E_y and H_y are solutions of the field propagation equations [5]. α_n and β are the spectral parameter and the phase constant, respectively, with $\epsilon_{ci} = \epsilon_{xi} = \epsilon_{zi}$ and $\mu_{ci} = \mu_{xi} = \mu_{zi}$. The index \sim represents the Fourier transform following x .

The following step was to use boundary conditions at all dielectric interfaces H_i to express the tangential electric field components (E_z , E_x) in terms of the currents densities J_x and J_z on the metallized interface H_m in the spectral domain. This allowed evaluating the admittance Green's dyadic functions:

$$\begin{bmatrix} \tilde{J}_x(\alpha_n) \\ \tilde{J}_z(\alpha_n) \end{bmatrix} = \begin{bmatrix} Y_{11} & Y_{12} \\ Y_{21} & Y_{22} \end{bmatrix} \begin{bmatrix} \tilde{E}_x \\ \tilde{E}_z \end{bmatrix} \quad (2)$$

and then, deducing the impedance form of the dyadic Green's matrix $[G]$ by a simple inversion of matrix $[Y]$.

A. Resolution by Galerkin Technique

The Galerkin's procedure is a particular case of the moment method where trial functions are equal to basis functions. In this technique, the tangential components J_x and J_z of the current density on each conductor strip are expanded onto two complete sets of P and Q basis functions, respectively:

$$J_{x,k} = \sum_{p=1}^P a_{p,k} J_{xp,k} \quad \text{and} \quad J_{z,k} = \sum_{q=1}^Q b_{q,k} J_{zq,k} \quad (3)$$

with $a_{p,k}$ and $b_{q,k}$ the real unknown coefficients to evaluate, with $k=1, 2$ (left or right strip conductor of the coupler, respectively).

First, the Fourier transforms of (3) are evaluated and substituted into (2). Next, after using the inner product with trial functions, the Parseval's identity as well as the

complementarity relations between the current and electric field on the two strips, we obtained an algebraic system of $2(P+Q)$ homogeneous linear equations in terms of the $2(P+Q)$ unknown coefficients $a_{p,k}$ et $b_{q,k}$ ($k=1, 2$).

$$\begin{bmatrix} [C_{11}(\omega, \beta)] & [C_{12}(\omega, \beta)] & [C_{13}(\omega, \beta)] & [C_{14}(\omega, \beta)] \\ [C_{21}(\omega, \beta)] & [C_{22}(\omega, \beta)] & [C_{23}(\omega, \beta)] & [C_{24}(\omega, \beta)] \\ [C_{31}(\omega, \beta)] & [C_{32}(\omega, \beta)] & [C_{33}(\omega, \beta)] & [C_{34}(\omega, \beta)] \\ [C_{41}(\omega, \beta)] & [C_{42}(\omega, \beta)] & [C_{43}(\omega, \beta)] & [C_{44}(\omega, \beta)] \end{bmatrix} \begin{bmatrix} a_{p1} \\ a_{p2} \\ b_{q1} \\ b_{q2} \end{bmatrix} = \vec{0} \quad (4)$$

The above homogeneous system was then solved for the phase constant β at each frequency f by setting the determinant of the matrix $[C_{j,m}(\omega, \beta)]$ ($j, m=1 \dots 4$) to zero and by seeking the roots of the resulting equation.

B. Basis functions choice criterias

An adequate choice of basis functions is essential to assure a reliable solution with minimum numerical treatments and processing time. Indeed, a suitable choice of basis functions leads to a better configuration of the current density on the strips. This choice must respect several convergence criteria as detailed in [6]. Convergence may be speeded up by using basis functions whose behaviors resemble the physical distribution. Sinusoidal trial functions with metallic edge singularities have been chosen for the general nonsymmetrical case [7]:

$$\begin{cases} J_{px1}(x) = \sin\left(\frac{p\pi(x-C_1)}{w_1}\right) & x \in [C_1, C_1 + w_1] \\ J_{px2}(x) = \sin\left(\frac{p\pi(x-C_2)}{w_2}\right) & x \in [C_2, C_2 + w_2] \end{cases}$$

$$\begin{cases} J_{qz1}(x) = \frac{\cos\left(\frac{(q-1)\pi(x-C_1)}{w_1}\right)}{\sqrt{\left(\frac{w_1}{2}\right)^2 - (x-C_1 - \frac{w_1}{2})^2}} & x \in [C_1, C_1 + w_1] \\ J_{qz2}(x) = \frac{\cos\left(\frac{(q-1)\pi(x-C_2)}{w_2}\right)}{\sqrt{\left(\frac{w_2}{2}\right)^2 - (x-C_2 - \frac{w_2}{2})^2}} & x \in [C_2, C_2 + w_2] \end{cases}$$

Note that the solution accuracy for β can be systematically enhanced by increasing the number of basis functions.

III. NUMERICAL RESULTS AND DISCUSSIONS

To confirm the adequate choice of basis functions, we analyzed a bilayer nonsymmetrical shielded coupler. Figures 2 and 3 show the convergence of the effective permittivity versus the total number of basis functions N_{fb} (equal to $2*(P+Q)$) and the total number of Fourier terms N_{tf} . Note that 100 Fourier terms and about 8 basis functions were sufficient to achieve a good convergence.

Moreover, we note that narrow strips ($w_1 = w_2 = 0.18\text{mm}$) require more spectral terms compared to wide ones ($w_1 = w_2 = 0.36\text{mm}$). A good compromise was found between accuracy, CPU time and memory storage with regard to differential methods since 4 basis functions per current density components were sufficient to reach convergence. Compared to differential methods which require a very dense mesh for a very good accuracy resulting on a large CPU time (as finite element method or FDTD method), the proposed technique is faster with a minimum memory storage.

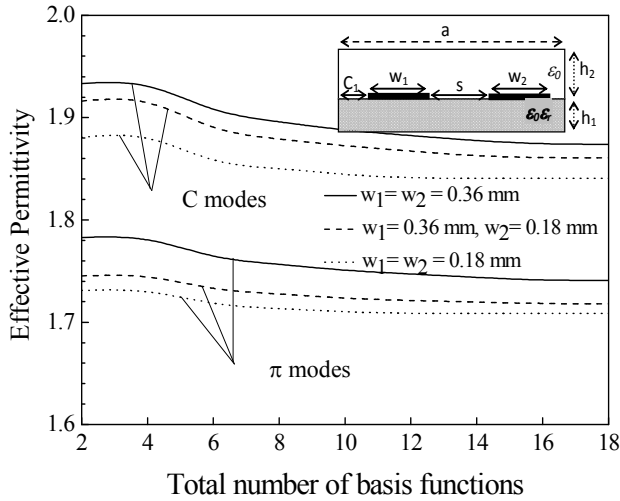


Figure 2. Convergence of the effective permittivity versus Nfb ($a=3.556\text{ mm}$, $S=0.45\text{ mm}$, $h_1=0.254\text{ mm}$, $h_2=6.858\text{ mm}$, $C_1=0.5\text{ mm}$, $\epsilon_r=2.22$, $f=10\text{ GHz}$, $N_{tf}=500$)

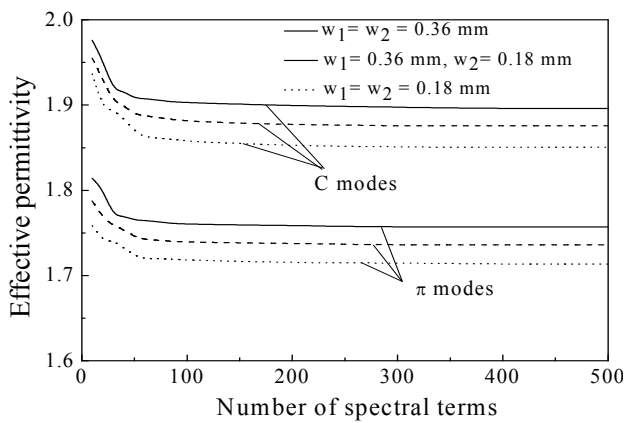


Figure 3. Convergence of the effective permittivity versus Ntf ($a=3.556\text{ mm}$, $S=0.45\text{ mm}$, $h_1=0.254\text{ mm}$, $h_2=6.858\text{ mm}$, $C_1=0.5\text{ mm}$, $\epsilon_r=2.22$, $f=10\text{ GHz}$, $N_{fb}=16$)

Figure 4, showing the variation of the determinant of $C_{ij}(\beta)$, demonstrates the simultaneous existence of two distinct solutions for β , very similar to those published in [7]. Note that the authors in [7] used the resonance transverse method (TRM), generally used to get the wave propagation constant in waveguides including dielectric ones. It takes advantage of the fact that a standing wave is present along a certain direction (transverse with respect to the main propagation direction), due to purely reactive loads at both ends of the transmission line (which

represents the wave propagation). Compared to TRM which is an integral method, the CPU time was reduced of about 20% depending of spectral terms N_{tf} and the number of basis functions N_{fb}

Figure 5 shows the variation of the effective permittivity ϵ_{eff} for different values of h_1 . The results agree well with [7]. The evolution of the effective permittivity is characterized by the existence of three regions: first, ϵ_{eff} decreases with h_1 for both c and π modes, this can be explained by the high concentration of fields in the thin substrate (near horizontal walls of the shield). Then, ϵ_{eff} reaches a constant value of about 1.6 corresponding to equal thicknesses between the substrate and the air region.

Finally, ϵ_{eff} decreases from $h_1 = 6.6\text{mm}$, due to the larger thickness of the substrate. The effective permittivity is higher for the lowest values of the substrate thickness.

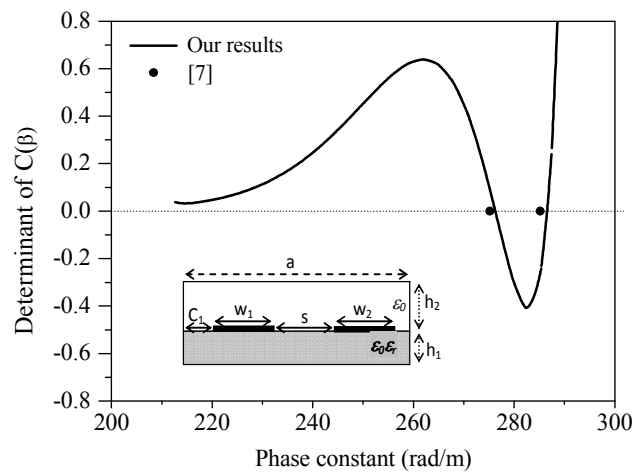


Figure 4. Determinant of $C(\beta)$ versus phase constant β ($a=3.556\text{ mm}$, $S=0.45\text{ mm}$, $h_1=0.254\text{ mm}$, $h_2=6.858\text{ mm}$, $W_1=W_2=0.36\text{ mm}$, $C_1=0.5\text{ mm}$, $\epsilon_r=2.22$, $f=10\text{ GHz}$)

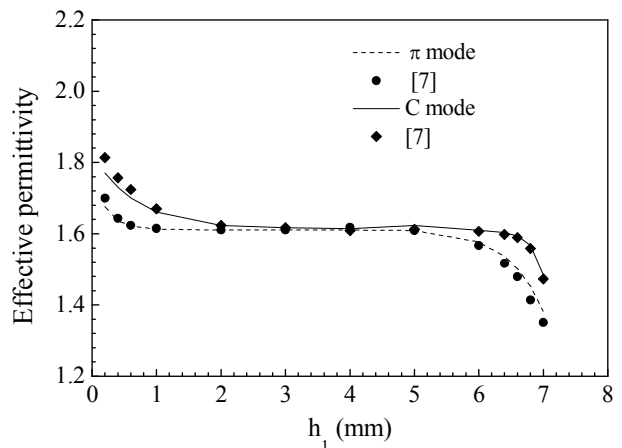


Figure 5. Permittivity versus h_1 ($a=3.556\text{ mm}$, $h_1+h_2=7.112\text{ mm}$, $w_1=0.08\text{ mm}$, $w_2=4w_1$, $S=0.45\text{ mm}$, $C_1=0.9\text{ mm}$, $\epsilon_r=2.22$, $f=10\text{ GHz}$)

Table I shows the effective permittivity of both even and odd modes for a coupled structure on epsilam 10 substrate. The relative average error is estimated to 1.5% for the odd mode and about 2% for the even mode.

TABLE I. VARIATION OF EFFECTIVE PERMITTIVITY VERSUS w/h_1 ($h_1=1mm, h_2=9mm, S=0.1mm, a=50mm, f=100 MHz, \epsilon_c=13, \epsilon_y=10.3$)

w/h	odd	odd [8]	even	even [8]
0.1	6.29	6.29	7.02	6.83
1	6.49	6.38	7.69	7.57
3	7.01	6.82	7.98	8.13

Figure 6 shows a comparison of dispersion charts between two anisotropic couplers using epsilam 10 substrate ($\epsilon_x=\epsilon_z=13, \epsilon_y=10.3$) and niobate lithium ($\epsilon_x=\epsilon_z=28, \epsilon_y=43$), respectively. Note that the phase constant is greater for lithium niobate due to higher field concentration.

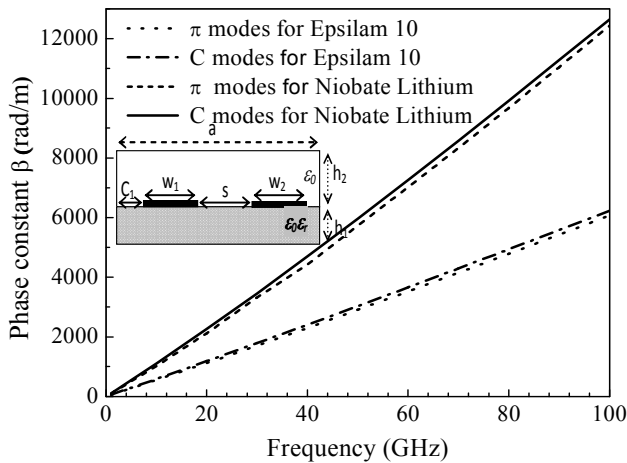


Figure 6. Dispersion chart for two anisotropic materials: Epsilam10 and niobate lithium. ($a=3.556 mm, S=0.45 mm, h_1=0.254 mm, h_2=6.858 mm, w_1=w_2=0.36 mm, C_1=0.5 mm$).

Figure 7 illustrates the variation of the guided wavelength λ_g versus frequency for a three-layer anisotropic coupler ($\epsilon_x=\epsilon_z=28, \epsilon_y=43$) and a bilayer isotropic coupler.

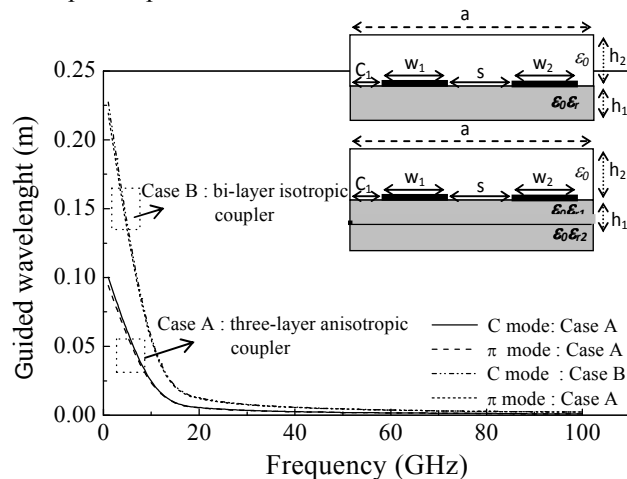


Figure 7. Comparison between a three-layer anisotropic coupler and a bilayer isotropic coupler ($a=3.556 mm, S=0.45 mm, h_1=0.254 mm, h_2=6.858 mm, w_1=w_2=0.36 mm, C_1=0.5 mm$, isotropic: $\epsilon_r=2.22$, Sapphire ($\epsilon_x=\epsilon_z=9.6, \epsilon_y=11.6$) and Epsilam10 ($\epsilon_x=\epsilon_z=13, \epsilon_y=10.3$).

The curves show that λ_g is always smaller for the three-layer coupler than for the bi-layer, thus allowing reducing the device size.

IV. CONCLUSION

This paper highlights an efficient and fast way to determine the fullwave numerical solutions required in multilayered coupled microstrip line analysis with arbitrary located metallic strips. Such devices are used in various applications in microwave integrated circuits, particularly in wireless communication, multiplexors, shifters, and delay lines, to name a few. To achieve this aim, we used the spectral domain technique via an adequate choice of basis functions for c- and π -modes through the Galerkin's procedure. The computed results are in good agreement with data available in the literature. The proposed CAD approach should be useful in high frequencies where the dispersion effects cannot be neglected.

REFERENCES

- [1] T.C. Edwards and M.B. Steer, Foundations of Interconnect and Microstrip Design, Chichester, England: Wiley and Sons, 2000.
- [2] K. Wincza and S. Gruszczynsky, "Asymmetric coupled line directional couplers as impedance transformers in balanced and η -way power amplifiers", IEEE Trans. Microwave Theory Tech., vol. 59, Jul. 2011, pp. 1803-1810.
- [3] A. Khodja, R. Touhami, M.C.E. Yagoub, and H. Baudrand, "Full-wave mode analysis of asymmetric coupled microstrip structures: particular case of quasi-symmetric lines", 27th Progress In Electromagnetics Research Symposium, Mar. 2011, pp. 176-180.
- [4] T. Itoh, "Spectral domain immittance approach for dispersion characteristics of generalized printed transmission lines", IEEE Trans. Microw. Theory Tech., vol. 28, Jul. 1980, pp.733 -736.
- [5] M.L. Tounsi, R. Touhami, and M.C.E. Yagoub, "Generic spectral immittance approach for fast design of multilayered bilateral structures including anisotropic media," IEEE Microwave and Wireless Components Letters, vol. 17, Jun. 2007, pp. 409-411.
- [6] A. Khodja, R. Touhami, M.C.E. Yagoub, and H. Baudrand, "Full-wave modal analysis of asymmetric coupled-lines using the quasi-symmetric approach", Mediterranean Microwave Symp., Sept. 2011, pp. 142-144.
- [7] A. Khodja, M.C.E. Yagoub, R. Touhami, and H. Baudrand, "Efficient characterization of millimeter-wave asymmetric coupled microstrip structures using the quasi-symmetric approach", International Journal of RF and Microwave CAE, Ed. Wiley, vol.23, Issue 5, Sept. 2013, pp. 527-538.
- [8] N.G. Alexopoulos, "Integrated circuit structures on anisotropic substrates, IEEE Trans. Microwave Theory Tech., vol. 33, Oct. 1985, pp 847-881.